

Stability of strained heteroepitaxial systems in $(1 + 1)$ dimensions

Pierre Thibault*

*Département de physique et Regroupement québécois sur les matériaux de pointe (RQMP)
Université de Montréal, Case Postale 6128, Succursale centre-ville, Montréal, Québec, Canada, H3C 3J7*

Laurent J. Lewis†

*Département de physique and Regroupement québécois sur les matériaux de pointe (RQMP)
Université de Montréal, Case Postale 6128, Succursale centre-ville, Montréal, Québec, Canada, H3C 3J7*

(Dated: December 17, 2018)

We present a simple analytical model for the determination of the stable phases of strained heteroepitaxial systems in $(1 + 1)$ dimensions. In order for this model to be consistent with a subsequent dynamic treatment, all expressions are adjusted to an atomistic Lennard-Jones system. Good agreement is obtained when the total energy is assumed to consist of two contributions: the surface energy and the elastic energy. As a result, we determine the stable phases as a function of the main “control parameters” (binding energies, coverage and lattice mismatch). We find that there exists no set of parameters leading to an array of islands as a stable configuration. We however show that a slight modification of the model can lead to the formation of stable arrays of islands.

PACS numbers: 68.35.-p, 68.43.Hn, 68.65.-k, 68.65.Hb

I. INTRODUCTION

It appears today that self-assembly is not only one of the most elegant avenues for the production of devices based on quantum dots (QD), but also one of the most promising. Basic understanding of the physics of the formation of arrays of islands should ultimately lead to the realization of such exciting concepts as spintronics^{1,2} and quantum dot cellular automata.³ Driven by these possible developments, considerable effort has been devoted to understanding and predicting the conditions necessary for ensuring the stability of arrays of islands. Simple arguments based on the scaling of the energy as a function of the volume of the islands⁴ indicate that any system naturally undergoes ripening and, therefore, the only relevant observation is the (very long) time scale needed for the system to reach equilibrium.⁵ It is becoming clear, however, that a realistic energy function can lead to arrays of islands as equilibrium configurations,^{4,6,7,8,9} as can also be deduced from experiment (see, e.g., Ref. 10 for a review).

The dynamics of formation of arrays of islands has to some extent been investigated using atomistic models,^{11,12,13,14} but is not yet fully understood. For instance, the importance of nucleation in the early stage of array formation is still unclear.¹⁵ The long-term goal of our work is to address such questions and to provide a coherent picture of island formation in heteroepitaxial systems, duly taking into account changes in the energy landscape arising from the lattice mismatch between the two components of the system. We aim to achieve this using a kinetic Monte Carlo (KMC) model, whereby the particles evolve according to the relative probabilities for hopping from one site to a neighbouring site on a fixed lattice. The main difficulty of this approach, which we are still in the process of developing, resides in properly modulating the energy barriers to account for elastic con-

tributions generated by the lattice mismatch between the two species. We note that this problem could in principle be approached using molecular dynamics (MD). However, the timescales involved in the present problem are such that MD calculations are not feasible at this time.

For lack of an accurate model for the kinetics of island formation, there is definite interest in the investigation of the equilibrium properties of heteroepitaxial systems, i.e., the surface morphology as determined by the various parameters that control the physics of the systems (lattice mismatch, coverage, binding energies, etc.). Our objective here is to present and discuss a continuous model suited for this purpose. This will enable us, in particular, to identify the regions of parameter space where the formation of stable, coherent arrays of island are favored. We develop an analytical expression for the zero-temperature total energy of a strained array of islands. To ensure consistency, an important constraint on this model is that it should be expressed in terms of quantities that can be “exported” to a subsequent KMC model which will allow the dynamics to be investigated. We do this by assuming Lennard-Jones interactions between the two types of atoms and considering a triangular “ $(1 + 1)$ -dimensional” geometry. This defines a reference system (which we will call the *LJ system*) on which both the static and the dynamic models should be mapped. Note that we use the term “ $(1 + 1)$ -dimensional”, rather than “2-dimensional”, to indicate that one of the spatial dimensions is height (the z component), not to be confused with the usual two-dimensional case where atoms move in the xy plane.

We thus obtain an expression for the difference in energy ΔE between a system with a flat layer of adsorbed atoms and a system where islands have formed. For a given set of control parameters, this quantity is minimized with respect to the size of the islands, the distance between the islands, and the thickness of the wet-

ting layer, so as to determine the equilibrium state of the system. We find that good agreement between the LJ system and the continuous model can be achieved by considering only two contributions in ΔE : the surface energy and the elastic energy, the latter arising from both relaxation and substrate-mediated island-island interactions. This general approach is in many respects similar to that proposed by Combe et al.⁴ (CJB). Apart from the fact that our model allows the lattice misfit and the energy parameters to vary, the main differences lie in the details of the method, as discussed below.

An important conclusion of our work is that *no single set of control parameters* leads to an array of islands as a stable configuration. This is in contradiction with the results of CJB;⁴ the discrepancy arises from the arbitrariness in the choice of the parameter (z_0) which represents the characteristic length for the decay of the adsorption energy above the surface. If we relax the constraint on the choice of this parameter (i.e., consistency with the LJ model is not imposed), then stable arrays of islands are found, along with a “cracks” phase, made of flat islands that touch at their base.

II. THE MODEL

A. The LJ system

As mentioned above, the reference system consists of atoms occupying the sites of a (1+1)-dimensional triangular lattice and interacting via the Lennard-Jones potential:

$$U(r) = 4\epsilon \left[\left(\frac{\sigma}{r} \right)^{12} - \left(\frac{\sigma}{r} \right)^6 \right]. \quad (1)$$

The atoms are of two types: substrate (S) and adsorbate (A). Thus, there are three different types of interactions and six different Lennard-Jones parameters that define the total energy: $\{\sigma_{SS}, \sigma_{AA}, \sigma_{SA}\}$ and $\{\epsilon_{SS}, \epsilon_{AA}, \epsilon_{SA}\}$. Since one of the σ 's and one of the ϵ 's fix the length scale and energy scale, respectively, there are only four free parameters. This number can be reduced to three by applying the Lorentz-Berthelot combination rule:

$$\sigma_{SA} = \frac{1}{2}(\sigma_{SS} + \sigma_{AA}). \quad (2)$$

Hence, there is a single degree of freedom as far as length scales are concerned, which can be expressed in terms of the lattice mismatch α , defined as

$$\alpha = \frac{\sigma_{AA} - \sigma_{SS}}{\sigma_{SS}}. \quad (3)$$

The other two degrees of freedom are the binding energies between adsorbate atoms, ϵ_{AA} , and between adsorbate and substrate atoms, ϵ_{SA} . These parameters are independent and $\epsilon_{SA} > \epsilon_{AA}$ is the wetting condition.

In practical calculations, the LJ interaction must be cutoff at some distance r_c . The choice of r_c affects slightly the physical properties of the system, notably the equilibrium interatomic distance r_{eq} , the cohesive energy u_0 , and the elastic constants. (See Section IIB2 for details on the calculation of the elastic constants). Table I presents the dependence of these important quantities on the cutoff radius.

r_c	$r_{eq} (\sigma)$	$u_0 (\epsilon)$	$\mu = \lambda (\epsilon)$
1.000 (1)	1.1225	-3.000	31.18
1.732 (2)	1.1159	-3.222	33.48
2.000 (3)	1.1132	-3.319	34.49
2.646 (4)	1.1122	-3.356	34.87
3.000 (5)	1.1119	-3.364	34.96
∞	1.1115	-3.382	35.15

TABLE I: Computed values of some important quantities as a function of the cutoff distance r_c (and number of nearest-neighbor shells): r_{eq} is the equilibrium interatomic spacing in units of σ , u_0 is the cohesive energy in units of ϵ , and μ and λ are the two Lamé parameters (both are equal in this geometry).

B. The Continuous Model

As discussed in the Introduction, our purpose is to evaluate the energy difference between a system in which the adsorbate atoms form islands and one in which they form a uniform layer on top of the substrate:

$$\Delta E = E_{\text{island}} - E_{\text{layer}}. \quad (4)$$

This energy difference can be decomposed into surface and elastic contributions,

$$\Delta E = \Delta E_{\text{surface}} + \Delta E_{\text{elastic}}, \quad (5)$$

and is a function of the following parameters:

- α , the lattice mismatch;
- ϵ_{SS} , the binding energy between two atoms of the substrate;
- ϵ_{AA} , the binding energy between two atoms of the adsorbate;
- ϵ_{SA} , the binding energy between an atom of the substrate and an atom of the adsorbate;
- θ , the coverage, expressed in monolayers (ML);
- h , the height of the islands, expressed in ML;
- L , the width of the islands at their base;
- z , the thickness of the wetting layer, expressed in ML;

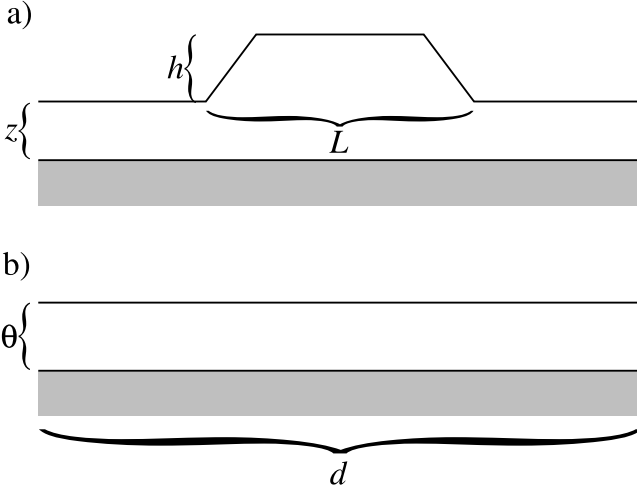


FIG. 1: Geometry of the system (a) with islands and (b) without islands. The shaded region is the substrate and the white region is the adsorbate. Islands are assumed to have the shape of an isosceles trapezoid, with contact angle $\frac{\pi}{3}$.

- d , the distance between the centers of two neighboring islands.

As mentioned earlier, one of the binding energies, say ϵ_{SS} , fixes the energy scale. The last five parameters describe the geometry of the system (cf. Fig. 1); they are integers but we will assume that they are real in order to facilitate the calculations. Since h , θ and z are expressed in ML, the actual height is obtained by multiplying by the thickness of one monolayer, $\frac{\sqrt{3}}{2}r_{eq}$.

The conservation of atoms (or volume) between the two configurations imposes a constraint on the geometric parameters:

$$\theta d = zd + h(L - h/2). \quad (6)$$

Since α , ϵ_{SS} , ϵ_{SA} , ϵ_{AA} and θ are assumed to be known from experiment for a given material, i.e., they can be considered as control parameters, the energy need only be minimised with respect to the three parameters L , h and z , d being determined by the constraint (6).

In the next two subsections we develop expressions for the two energy contributions in Eq. (5) as a function of the various parameters of the problem. They are derived largely from theoretical considerations but, in some cases, *ad hoc* terms are introduced in order to ensure that the model is consistent with the LJ system; in these cases, we proceed as follows: first, we generate a set of configurations with some number of adsorbate atoms placed in the shape of a trapezoid. Then, with suitably chosen parameters (ϵ and σ), we let the whole system (including a substrate large enough to make finite size effects negligible) relax to minimum energy. Periodic boundary conditions are used along the x direction. Figure 2 illustrates the atomic displacement of the atoms of an island as a result of relaxation.

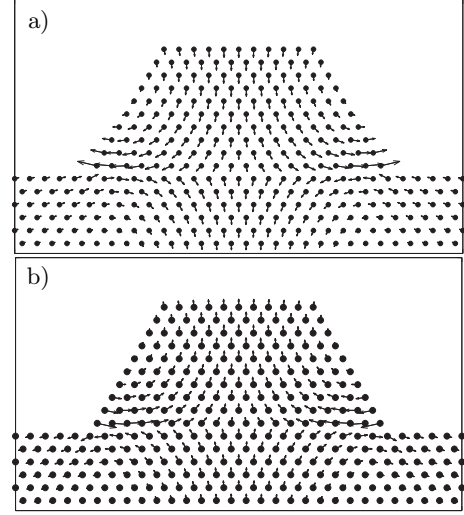


FIG. 2: Displacements of the atoms of a relaxed island ($L = 20, h = 10$). (a) tensile ($\alpha = -1\%$); (b) compressive ($\alpha = +1\%$). The lengths of the arrows are about 30 times the actual atomic displacements.

1. The Surface Energy

We first determine the adsorption energy of an island of type S (i.e., “substrate on substrate”) whose actual height is $h(x)$, or $\tilde{h}(x)$ when expressed in ML (see Fig. 3). This energy is the sum of bulk and surface contributions:

$$E_S^{\text{island}} = Vu_0\epsilon_{SS} + (\tilde{L} - L)\gamma_{SS}, \quad (7)$$

where V is the volume of the island, $u_0\epsilon_{SS}$ the cohesive energy per atom, $(\tilde{L} - L)$ the increase of surface due to the island, and γ_{SS} the surface energy density. Using $\tilde{L} = \int \sqrt{dx^2 + dz^2} = \int \sqrt{1 + h'^2(x)} dx$, E_S^{island} can readily be rewritten in terms of $\tilde{h}(x)$:

$$E_S^{\text{island}} = \int_0^L \left[\tilde{h}u_0\epsilon_{SS} + \left(\sqrt{\frac{3}{4}\tilde{h}'^2 + 1} - 1 \right) \gamma_{SS} \right] dx, \quad (8)$$

where the factor $\frac{3}{4}$ comes from the substitution of $h(x)$ by $\frac{\sqrt{3}}{2}\tilde{h}(x)$.

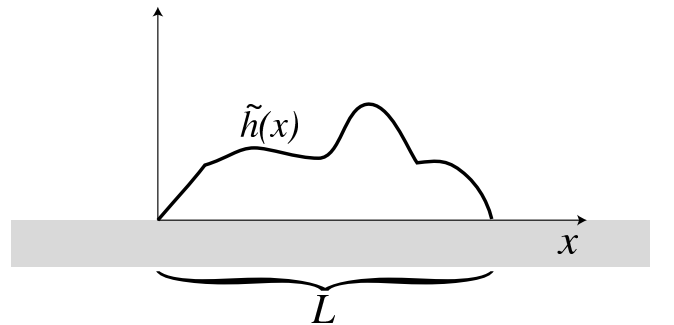


FIG. 3: Island of shape given by $\tilde{h}(x)$.

The surface energy density γ_{SS} is proportional to ϵ_{SS} ; we can write

$$\begin{aligned}\gamma_{SS} &= C\epsilon_{SS} \\ \gamma_{AA} &= C\epsilon_{AA} \\ \gamma_{SA} &= C(\epsilon_{SS} + \epsilon_{AA} - 2\epsilon_{SA}),\end{aligned}\quad (9)$$

where C is a constant that depends on the number of neighbors taken into account in the model.

If the island is of type A (i.e., adsorbate on substrate), now, the adsorption energy is easily obtained from Eq. (8) by substituting ϵ_{AA} and γ_{AA} for ϵ_{SS} and γ_{SS} and adding a term describing the interaction between the island and the substrate. If we assume nearest-neighbor interactions, this term involves only the atoms at the interface between the island and the substrate. In a more general situation, the adsorption energy for an atom at position z above the surface (in ML) can be written

$$E_{\text{ad}}(z) = E_{\text{ad}}^0 + (\epsilon_{AA} - \epsilon_{SA})\eta(z), \quad (10)$$

where E_{ad}^0 is the “generic” adsorption energy for the case $\epsilon_{SA} = \epsilon_{AA}$ and $\eta(z)$ is a function which decreases with z , with characteristic length z_0 . As in similar works^{4,7,16} we assume the form:

$$\eta(z) = Ae^{-z/z_0}; \quad (11)$$

the parameters A and z_0 can be determined by fitting to the total energy of a particular atomic model (here Lennard-Jones). Using (10), we find that the adsorption energy of a vertical column of h atoms is proportional to

$$\sum_{j=1}^h e^{-j/z_0} = \frac{1 - e^{-h/z_0}}{e^{1/z_0} - 1}. \quad (12)$$

Hence, we obtain:

$$\begin{aligned}E_A^{\text{island}} &= \int_0^L \left[\tilde{h}u_0\epsilon_{AA} + \left(\sqrt{\frac{3}{4}\tilde{h}^2 + 1} - 1 \right) \gamma_{AA} \right. \\ &\quad \left. + B(\epsilon_{AA} - \epsilon_{SA}) \left(1 - e^{-\tilde{h}/z_0} \right) \right] dx, \quad (13)\end{aligned}$$

where $B = A/(e^{1/z_0} - 1)$. It can easily be shown that $B = 2C$ by taking the limiting case of a very thick adsorbate. Overall, therefore, only two parameters need to be fitted to the atomic model, namely B and z_0 . This fit was carried out on systems with uniform adsorbed layers of thickness θ [i.e., $\tilde{h}(x) = \theta \Rightarrow \tilde{h}'(x) = 0$]. In this case, the energy difference between a system with an adsorbate of type A and an adsorbate of type S is

$$\begin{aligned}E_A^{\text{layer}} - E_S^{\text{layer}} &= d[\theta u_0(\epsilon_{AA} - \epsilon_{SS}) \\ &\quad + B(\epsilon_{AA} - \epsilon_{SA})(1 - e^{-\theta/z_0})]. \quad (14)\end{aligned}$$

The numerical calculations yield $B = 2.53$ and $z_0 = 0.39$ (see Appendix A for details).

Assuming $\tilde{h}(x)$ describes a trapezoidal shape, we can finally write the first term of (5) as

$$\begin{aligned}\Delta E_{\text{surface}} &= 2C(\epsilon_{AA} - \epsilon_{SA})[d - (d - L + z_0)e^{-z/z_0} \\ &\quad - (L - h - z_0)e^{-(h+z)/z_0} - d(1 - e^{-\theta/z_0})] + C\epsilon_{AA}h.\end{aligned}\quad (15)$$

2. Elasticity

It is an interesting fact that the theory of elasticity, which deals with continuous media, can accurately describe systems as small as a few tens or hundreds of atoms (see Ref. 17 for instance). In this work, we exploit this property to construct (at least in part) the analytical expressions entering the second term of (5). Unfortunately, we know of no analytical solution to the elasticity differential equations for a system with the boundary conditions illustrated in Fig. 1a). This difficulty can be circumvented by making some assumptions on the force distribution caused by the island on the substrate. As argued by Tersoff and Tromp,¹⁸ when the island is very flat ($h \ll L$), one can assume that there is no strain relaxation in the z direction. This leads to a force distribution which is proportional to the derivative of the height function, $f \propto h'(x)$. In more general cases, however, we found that a (truncated) linear force density was a better assumption. Since higher islands deform the substrate more efficiently (for a given volume), we used the following expression:

$$f(x) = \begin{cases} kx & \text{if } |x| < \frac{L}{2} \\ 0 & \text{otherwise,} \end{cases} \quad (16)$$

where k is a constant (to be determined) which depends on the lattice mismatch, the shape of the island and the elastic moduli of both the island and the substrate.

Following the guidelines presented in Ref. 19, we find that the Green's tensor for a semi-infinite two-dimensional plane is

$$\begin{aligned}G_{xx} &= \frac{(\lambda + \mu)x^2 - (\lambda + 2\mu)r^2 \log(r)}{2\pi\mu(\lambda + \mu)r^2} \\ G_{xz} &= \frac{(\lambda + \mu)xz - \mu r^2 \arctan(\frac{x}{z})}{2\pi\mu(\lambda + \mu)r^2} \\ G_{zx} &= \frac{(\lambda + \mu)xz + \mu r^2 \arctan(\frac{x}{z})}{2\pi\mu(\lambda + \mu)r^2} \\ G_{zz} &= \frac{-(\lambda + \mu)x^2 - (\lambda + 2\mu)r^2 \log(r)}{2\pi\mu(\lambda + \mu)r^2},\end{aligned}\quad (17)$$

where $r^2 = x^2 + z^2$. The x component of the displacement field on the surface of the substrate is found to be

$$\begin{aligned}u_x(x, z=0) &= \int_{-\infty}^{\infty} G_{xx}(x, z=0)f(x-x')dx' \\ &= \frac{L}{2}\tilde{u}\left(\frac{2x}{L}\right),\end{aligned}\quad (18)$$

where $\tilde{u}(\xi)$ is a scale-independent function:

$$\tilde{u}(\xi) = \kappa \left[2\xi + (1 - \xi^2) \log \left| \frac{1 + \xi}{1 - \xi} \right| \right], \quad (19)$$

with $\kappa = \frac{3kL}{16\pi\mu_S}$ and μ_S is one of the Lamé parameters of the substrate.

Because the atoms lie on a triangular lattice and interact via a radial potential, the two Lamé parameters μ and λ must be equal, given by

$$\lambda = \mu = \frac{\sqrt{3}}{8} \sum_j r_j^2 U''(r_j), \quad (20)$$

the sum being carried out over all lattice points within a given cutoff radius. The Young modulus and Poisson ratio for a 2-dimensional system are²⁴

$$\begin{aligned} E &= \frac{4\mu(\lambda + \mu)}{\lambda + 2\mu} = \frac{8}{3}\mu \\ \nu &= \frac{\lambda}{\lambda + 2\mu} = \frac{1}{3}. \end{aligned} \quad (21)$$

With these assumptions, we can construct expressions for the two principal elastic contributions to the total energy arising from the presence of a mismatched island on a substrate, viz. the energy due to the mutual strain between the island and the substrate, and the island-island interaction energy mediated by the substrate:

$$\Delta E_{\text{elastic}} = \Delta E_{\text{strain}} + E_{\text{interaction}}. \quad (22)$$

The elastic energy per unit volume (more precisely unit area in the present case) of a strained uniform adsorbed layer is

$$\frac{dE_{\text{elastic}}^{\text{layer}}}{dV} = \frac{1}{2} E_A \alpha^2, \quad (23)$$

E_A being the Young modulus of the adsorbate. Hence, a portion of width d of this $\frac{\sqrt{3}}{2}\theta$ -thick layer has an energy

$$E_{\text{elastic}}^{\text{layer}} = \frac{2}{\sqrt{3}} \mu_A \alpha^2 \theta d. \quad (24)$$

Similarly, we can write

$$E_{\text{elastic}}^{\text{island}} = \frac{1}{2} E_A \alpha^2 v(L, h), \quad (25)$$

where $v(L, h)$ is a function (to be determined) having units of volume. CJB⁴ write this as

$$v(L, h) = R(r)V, \quad (26)$$

where $r = h/L$ is the aspect ratio, V is the volume of the island, and $R(r)$ is a dimensionless function bounded between 0 and 1. Evidently, for scaling reasons, any $v(L, h)$ can be written in this form. In the present work, however, we choose to determine $v(L, h)$ without invoking

this scaling ansatz. This choice is mainly dictated by accuracy considerations: in order to fit $R(r)$ to numerical data, it is necessary to divide the computed elastic energy by the volume, thereby reducing the relative importance of large islands (see appendix B for more details).

We find that an excellent fit to the Lennard-Jones data is obtained with

$$v(L, h) = \frac{\sqrt{3}}{2} \frac{L^2}{c} \left[1 - e^{-ch/(L-h)} \right], \quad (27)$$

where c is the only (unitless) parameter to be adjusted to the data. Numerical calculations on the LJ system yield $c = 13.5$ (see Appendix A for details). Ratsch and Zangwill²⁰ have developed a similar function from theoretical considerations; the only difference is the denominator of the exponent, where they use L instead of $L - h$ and find $c = 2\sqrt{3}\pi \approx 10.9$.

In summary we have, for the elastic energy due to the strain between the island and the substrate:

$$\Delta E_{\text{strain}} = \frac{2}{\sqrt{3}} \mu_A \alpha^2 \left[\frac{L^2}{c} \left(1 - e^{-ch/(L-h)} \right) + zd - \theta d \right], \quad (28)$$

where we include the contribution arising from the presence of a wetting layer of thickness z in the system with islands.

The substrate-mediated interaction energy between two islands a distance d apart — the second term in Eq. (22) — can be written as a surface integral,

$$E_{\text{isl-isl}}(d) = \int_{-\infty}^{\infty} u_x(x) f(x - d) dx, \quad (29)$$

where $u_x(x)$ is the displacement field of the first island and f is the surface force distribution of the second island. Using (16) and (19), we get:

$$\begin{aligned} E_{\text{isl-isl}}(d) = & -\frac{4\pi\mu_S\kappa^2}{pL^2} \left[3L^4 + 2d^2L^2 + 4dL^3 \log \left| \frac{d-L}{d+L} \right| \right. \\ & \left. + 2(d^4 - 3d^2L^2) \log \left| \frac{d^2 - L^2}{d^2} \right| \right]. \end{aligned} \quad (30)$$

Note that this expression remains finite when $d \rightarrow L$. Since we are interested in the interaction energy for an array of islands, we have to sum up all contributions coming from the islands at position $\dots, -2d, -d, d, 2d, \dots$. In order to get a simple expression for our model, we may replace $E_{\text{isl-isl}}$ by the first few terms of its asymptotic series,

$$E_{\text{isl-isl}} \approx \frac{2\pi^2\mu_S L^2 \kappa^2}{9} \left(\frac{2L^2}{3\pi d^2} + \frac{L^4}{5\pi d^4} + \frac{3L^6}{35\pi d^6} + \dots \right). \quad (31)$$

The sum of all possible contributions can now be carried

out exactly:

$$E_{\text{interaction}} = \sum_{\substack{j=-\infty \\ j \neq 0}}^{\infty} E_{\text{isl-isl}}(j d) \approx \frac{4\pi^3 \mu_S L^2 \kappa^2}{81} \left(\frac{L^2}{d^2} + \frac{\pi^2 L^4}{50 d^4} + \frac{\pi^4 L^6}{1225 d^6} \right). \quad (32)$$

We still have to determine the dependence of κ [cf. Eq. (19)] on the parameters of our model. Let us first recall that this quantity is proportional to the amplitude of the force distribution exerted on the substrate by the island and, therefore, it also determines the amplitude of the displacement field in the substrate. We assume κ to have the following form:

$$\kappa = \alpha \kappa_\mu(\mu_A, \mu_S) \kappa_{\text{geo}}(h, L), \quad (33)$$

where κ_μ depends only on the elastic coefficients of the substrate and the adsorbate, and κ_{geo} depends only on the geometry of the island. κ is linear in α because Eq. (19) has itself been derived within the framework of the linear theory of elasticity.

For κ_μ we propose the *ad hoc* expression

$$\kappa_\mu = \frac{\mu_A}{\mu_A + \mu_S} \quad (34)$$

which satisfies the three important limiting cases

$$\begin{aligned} \mu_S \gg \mu_A &\implies \kappa_\mu \rightarrow 0 \\ \mu_S \ll \mu_A &\implies \kappa_\mu \rightarrow 1 \\ \mu_S = \mu_A &\implies \kappa_\mu = \frac{1}{2}. \end{aligned} \quad (35)$$

The first relation corresponds to the case of a substrate which is much more rigid than the adsorbate, the second is the opposite case, and the third is the case of equally rigid substrate and adsorbate. The geometry factor κ_{geo} can be determined by fitting to the LJ data. We find the following expression to yield good results:

$$\kappa_{\text{geo}} = \frac{1}{4} \left(1 - e^{-a_1 L + a_2} \right) \left(1 - e^{-b_1 h / (L-h) + b_2} \right). \quad (36)$$

The first factor, $\frac{1}{4}$, is such that $\partial_x u_x$, the x -component of the substrate's strain tensor, is always between 0 and α . The second factor ensures that κ_{geo} goes rapidly to 1 when L is larger than a few atoms. The last factor is a scale invariant term which is maximum when the aspect ratio $\frac{h}{L}$ is 1. After fitting the displacement field to the LJ data (see Appendix A), we find the following set of values for the parameters entering the above expression:

$$\begin{aligned} a_1 &= 12.6/r_{\text{eq}}, & a_2 &= 0.028, \\ b_1 &= 0.033, & b_2 &= -1.35, \end{aligned} \quad (37)$$

where r_{eq} is the equilibrium interatomic distance (see previous section).

Putting everything together, we obtain the following long expression for the interaction energy in Eq. (22):

$$E_{\text{interaction}} = \frac{4\pi^3 \mu_S L^2}{81} \left[\frac{\alpha}{4} \frac{\mu_A}{\mu_A + \mu_S} \left(1 - e^{-a_1 L + a_2} \right) \left(1 - e^{-b_1 h / (L-h) + b_2} \right) \right]^2 \left(\frac{L^2}{d^2} + \frac{\pi^2 L^4}{50 d^4} + \frac{\pi^4 L^6}{1225 d^6} \right). \quad (38)$$

We are now in position to construct the phase diagram of our model as a function of the various control parameters.

III. RESULTS AND DISCUSSION

A. Phase Diagrams

The energy difference ΔE between a system in which the adsorbate atoms form islands and a system in which they form a uniform layer on top of the substrate, Eq. (4), can be expressed as

$$\Delta E = \Delta E_{\text{surface}} + \Delta E_{\text{strain}} + E_{\text{interaction}}, \quad (39)$$

where the three terms are given by Eqs. (15), (28), and (38), respectively. We now proceed to determine the equilibrium configurations of the system as a function of the control parameters, viz. binding energies, mismatch and coverage. The parameter space is sampled as follows:

$$\begin{aligned} \epsilon_{AA} &= 0.7, 0.8, \dots, 1.2, 1.3 \\ \epsilon_{SA} &= 0.7, 0.8, \dots, 1.2, 1.3 \\ \alpha &= 0\%, 1\%, \dots, 9\%, 10\% \\ \theta &= 1, \dots, 14, 15, \end{aligned}$$

and $\epsilon_{SS} = 1$ sets the energy scale. We took positive values of α only since ΔE depends quadratically on this parameter. For every possible combination of the above parameters, we determine h , L , d and z such that ΔE is minimal. If the minimum ΔE is larger than zero, the

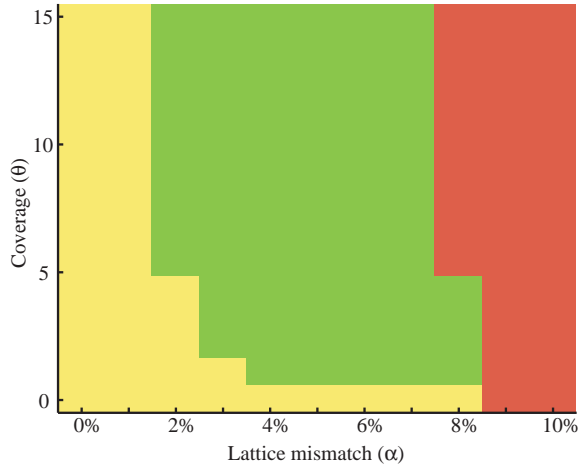


FIG. 4: (Color online) A typical phase diagram; here $\epsilon_{AA} = 1$ and $\epsilon_{SA} = 1.1$. The three phases are: ■ Frank-van der Merwe; ■ ripening islands with wetting layer; ■ ripening islands without wetting layer.

equilibrium configuration is a uniform adsorbate layer on the substrate; this phase is known as the “Frank-Van der Merwe” phase. If it is less than zero, the equilibrium phase depends on the values of h_{\min} , L_{\min} , d_{\min} , and z_{\min} which minimize ΔE . A few different situations can arise (we omit the “min” subscript to facilitate reading):

1. If $d \rightarrow \infty$, the islands undergo ripening, either directly on the substrate ($z = 0$) or on a wetting layer ($z \neq 0$);
2. If d is finite and $L < d$, the equilibrium configuration is an array of islands either on the substrate (“Volmer-Weber” phase²²) or on a wetting layer (“Stranski-Krastanov” phase²³).
3. If d is finite and $L = d$, the system is “cracked”, that is, islands touch at their base.

Following the example of Daruka et al.⁷, we produce a set of phase diagrams in the α - θ plane. Figure 4 shows a typical phase diagram for specific values of the binding energies ($\epsilon_{AA} = 1$ and $\epsilon_{SA} = 1.1$). Such plots are collected in Fig. 5 for the whole array of values of ϵ_{AA} and ϵ_{SA} investigated.

We observe, first, that only one phase is possible when $\epsilon_{AA} > \epsilon_{SA}$ (above the main diagonal of the plot), namely ripening islands without wetting layer. This is not surprising since it corresponds to the non-wetting case in which all terms of ΔE but $E_{\text{interaction}}$ are negative. A more important conclusion that can be drawn from Fig. 5 is that *no set of control parameters leads to an array of islands as a stable configuration*. This is in disagreement with the results of CJB.⁴ The discrepancy can be traced back to the choice of z_0 , the characteristic length for the decay of the adsorption energy at the surface, discussed in Section II B 1. The value of this parameter (0.39) was

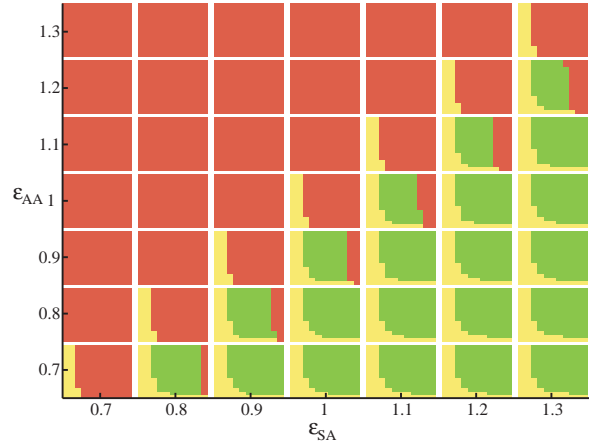


FIG. 5: (Color online) Phase diagrams for all values of the binding energies considered; here $\epsilon_{SS} = 1$ and $z_0 = 0.39$. Each small image is a phase diagram in the α - θ plane similar to that of Fig. 4. The colors correspond to the different phases: ■ Frank-van der Merwe; ■ ripening islands with wetting layer; ■ ripening islands without wetting layer.

obtained, in the present model, by fitting to the LJ potential, while CJB chose it in an *ad hoc* manner.

B. Extended model

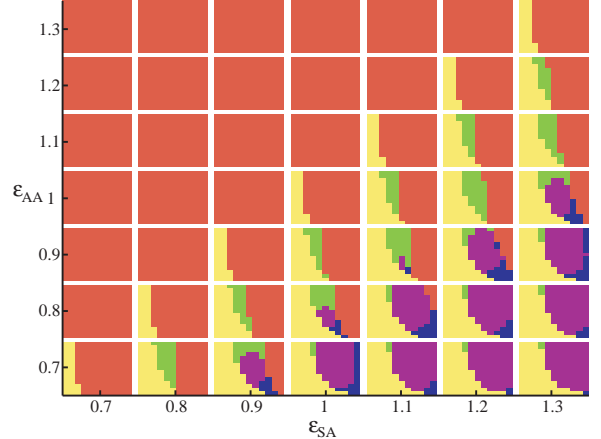


FIG. 6: (Color online) Same as Fig. 5, but for $z_0 = 3.0$. The various phases are as follows: ■ Frank-van der Merwe; ■ ripening islands with wetting layer; ■ ripening islands without wetting layer; ■ cracks; ■ Volmer-Weber.

We may relax the constraint on the value of z_0 for a moment and set $z_0 = 3$, close to the value used by CJB, resulting in an increase of the influence of the substrate on the adatoms higher above the interface. The introduction of this new length scale in the problem allows some new features to appear. The corresponding phase diagrams are displayed in Fig. 6. Consistent with CJB, we now observe the existence of two different stable

phases. In addition to the stable array of islands, we now find an equilibrium state consisting of islands touching at their base. Since this morphology is somewhat better described by a flat layer with very narrow troughs, we will refer to it as the “cracks” phase (shown in red in Fig. 6). The Stranski-Krastanov phase never appeared in the parameter space we considered.

It is not clear that potentials with $z_0 = 3$ do in fact exist, but it is certainly conceivable, in the case for instance of semiconductors, that the decay length of the surface energy is significantly larger than that of the LJ potential and, as a consequence, stable phases would exist. Consideration of this extended system is consistent with our long term objectives since z_0 can be included as an adjustable parameter in the KMC calculations.

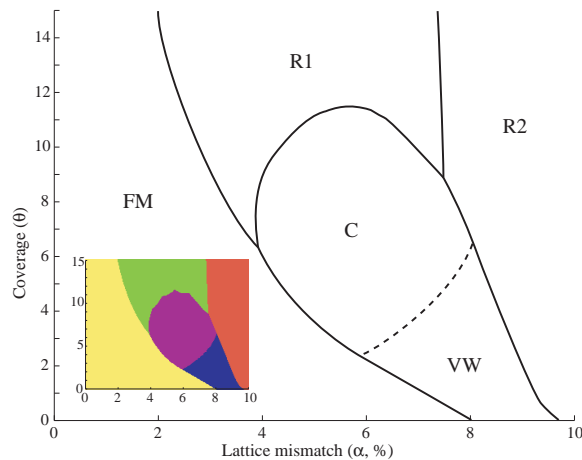


FIG. 7: (Color online) Phase diagram for the system with $z_0 = 3.0$, $\epsilon_{AA} = 1$, and $\epsilon_{SA} = 1.3$. The various phases are: Frank-van der Merwe (FM), ripening islands with wetting layer (R1), ripening islands without wetting layer (R2), cracks (C), and Volmer-Weber (VW). The dashed line indicates the smooth transition between the VW and the C phases. Inset: original phase diagram used to construct the main graph.

In order to get more detailed information about the stable phases, we selected one of the phase diagrams of Fig. 6 ($\epsilon_{SA} = 1.3$, $\epsilon_{AA} = 1$) and repeated the calculations on a finer grid (200×200). The resulting diagram is shown in Fig. 7. Note that, in this graph, the layout of the phase boundaries have been drawn as a “guide to the eye” using the original data (shown in the inset); we do not know the analytical form (if it exists) of these curves. (The slightly “zigzagging” behaviour of the boundary is a consequence of allowing z to take only integer values in the minimization process.) We find that the transition is not sharp between the Volmer-Weber (VW) and “cracks” (C) phases (hence the dashed line). Figure 7 has some features similar to the phase diagram computed by Daruka et al.⁷, in particular the shape of the FM, R1 and R2 phases.

The Frank-van der Merwe (FM) and the two ripening (R1 and R2) phases have no interesting intrinsic features; the first is flat, and the two others correspond to the

minimizing parameters going to infinity. We are therefore more concerned about the two stable phases (C and VW). A characteristic quantity often measured is the island density n on the surface. In our model, since the center-to-center distance between islands is d , we simply have $n = 1/d$. Figure 8 shows how the density varies as a function of coverage and lattice misfit for the binding energies selected. In the C phase, this density is simply the cracks density, that is, the number of cracks per unit length.

We have also computed the aspect ratio of the islands as a function of coverage and lattice mismatch; this is shown in Fig. 9. The global behavior is as expected: as α increases, the elastic relaxation process becomes more and more efficient and the islands can afford an increase of their surface; this explanation holds for the cracks phase as well.

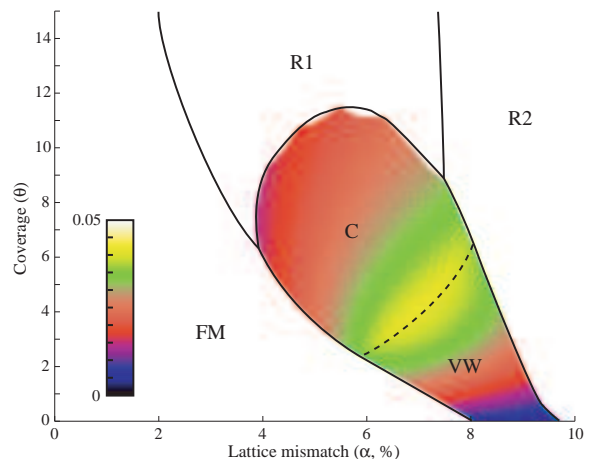


FIG. 8: (Color online) Island density $1/d$ in the two stable phases as a function of coverage θ and lattice mismatch α . Here, $z_0 = 3.0$, $\epsilon_{AA} = 1$, and $\epsilon_{SA} = 1.3$.

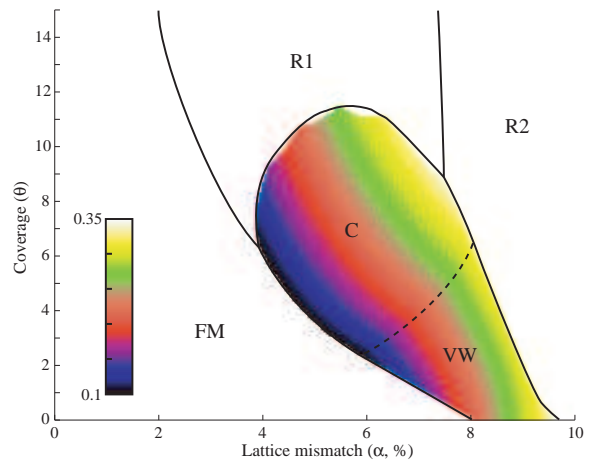


FIG. 9: (Color online) Aspect ratio h/L in the two stable phases as a function of coverage θ and lattice mismatch α . Here $z_0 = 3.0$, $\epsilon_{AA} = 1$, and $\epsilon_{SA} = 1.3$.

In both Figs. 8 and 9, the quantities shown by the color scale are conspicuously continuous at the VW-C boundary. This was to be expected since the very definition of these phases implies no jump in any quantity (VW phase for $L < d$, C phase for $L = d$). This boundary actually is the only second order phase transition; all others are first order.

To our knowledge, a cracks phase has never been reported. We do not know if an equivalent 3D phenomenon has been observed experimentally. In our model, the occurrence of such a phase is obviously related to the interaction energy term. Have we had assumed that $E_{\text{interaction}}$ is infinite when the islands touch (as did CJB⁴), the C phase would have been entirely precluded. A stronger island-island repulsion might also lead to the appearance of a Stranski-Krastanov (SK) phase for intermediate coverage. While it remains to be verified, we expect this cracks phase to be very close, at finite temperature for instance, to a SK phase; this is however beyond the scope of the present work.

IV. CONCLUSION

We have presented a simple analytical model for the determination of the stable phases of strained heteroepitaxial systems in $(1 + 1)$ dimensions. The model was developed with a view of carrying out KMC simulations of the dynamics of the formation of islands. This is a very difficult task, but already we have made progress in this direction, on which we will report in a subsequent publication. In order for the present model to be exportable to a KMC code, all expressions were adjusted to an atomistic Lennard-Jones system. The present calculations reveal that, for parameters which are consistent with the Lennard-Jones model, the array of islands is not a stable configuration of the system. If full consistency of the parameters is not imposed, and in particular if we relax the value of the decay length for the adsorption energy (z_0), then a stable array of islands arises. We argue that z_0 may in fact be viewed as an adjustable parameter, which can be used to describe systems other than Lennard-Jones, in particular semiconductors. Our calculations also reveal, in these conditions, the formation of a cracks phase — an array of islands touching at their base. While much work remains to be done, the present model is a first step in our aim of better understanding the formation of dislocation-free arrays of islands.

Acknowledgments

One of us (PT) is grateful to P. Jensen and J.-L. Barlat, from the “Laboratoire de physique de la matière condensée et nanostructures, Université Claude-Bernard Lyon-1”, for hospitality and fruitful discussions. This work was supported by grants from the Natural Sciences and Engineering Research Council (NSERC) of Canada

and the “Fonds québécois de la recherche sur la nature et les technologies” (FQRNT) of the Province of Québec. We are indebted to the “Réseau québécois de calcul de haute performance” (RQCHP) for generous allocations of computer resources.

APPENDIX A: COMPUTATIONAL DETAILS

We present here some details of the method used to fit the free parameters arising in the derivation of the continuous model presented in Section II.

In what follows, the cutoff radius of the potential has been fixed to $r_c = 3.2$, i.e., midway between the 5th and 6th neighbour shells. The equilibrium distance between substrate atoms is set to 1 so that $\sigma_{SS} = 1/1.1119 = 0.8993$ (cf. Table I). In all calculations, the substrate has thickness between 50 and 100 layers, with the lower three maintained fixed to mimic the presence of the bulk. For every configuration, the energy was determined by relaxing the positions of the atoms using a conjugate-gradient algorithm.

1. Surface Energy

The parameters B and z_0 in Eq. (13) have been fitted to systems composed of 50 substrate layers and coverage $\theta \in \{1, 2, 3, 4, 5, 10\}$. These configurations have been relaxed for a set of combinations of energy parameters $(\epsilon_{AA}, \epsilon_{SA}) \in \{0.8, 0.9, 1, 1.1, 1.2\}^2$. Altogether, the minimum total energies of 150 different systems have been computed. For every system, the difference between the total energy and the total energy of the equivalent system with $\epsilon_{SA} = \epsilon_{AA} = \epsilon_{SS}$ has been calculated. The numerical values for $E_A^{\text{layer}} - E_S^{\text{layer}}$ in (13) have then been fitted to an equation of the form

$$E_A^{\text{layer}} - E_S^{\text{layer}} = C_1(\theta)(\epsilon_{AA} - \epsilon_{SS}) + C_2(\theta)(\epsilon_{AA} - \epsilon_{SA}). \quad (\text{A1})$$

Figure 10 shows the dependence of C_1 and C_2 on coverage. C_1 is completely determined (i.e., there are no free parameters), given by $C_1 = du_0\theta$, where $u_0 = 3.364$ is the cohesive energy for a cutoff radius of 3 (see Table I). C_2 was fitted to a curve of the form $B(1 - e^{-\theta/z_0})$; the fit yields $B = 2.53$ and $z_0 = 0.39$.

2. Elastic Energy and Island-island Interaction Energy

The parameters a_1 , a_2 , b_1 , b_2 , and c of Eqs. (27) and (36) have been fitted to the same configurations as above. 30 different islands have been generated, of width L in the range 20 to 80 (six values) and height h in the range 1 to L (five values). Each of these configurations was relaxed with misfits of +1% and -1%. While the relaxed

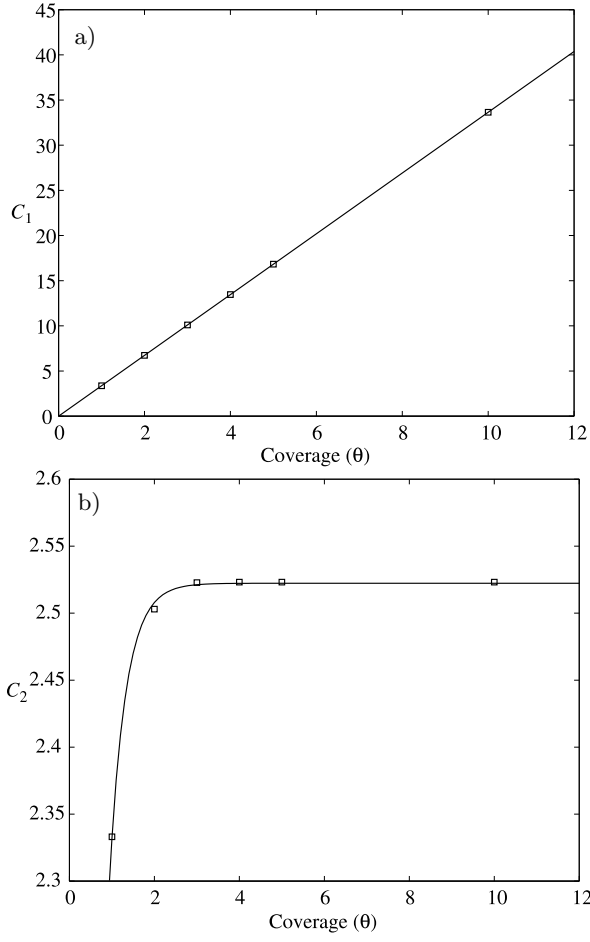


FIG. 10: Comparison between the numerical values of C_1 and C_2 (in equation A1) and the theoretical curves (see text). (a) The curve has no free parameter. (b) The curve is the best fit to the data.

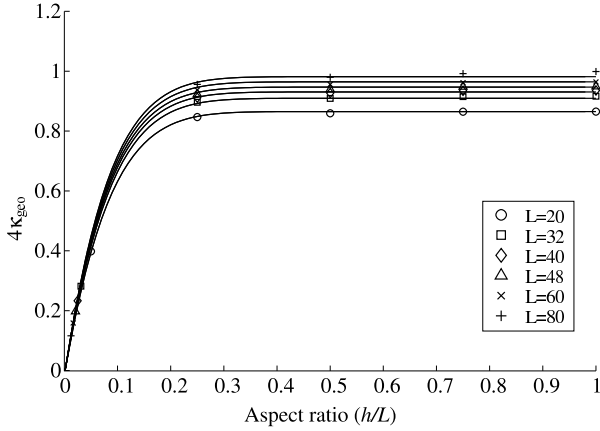


FIG. 11: Numerical data and theoretical curves for κ_{geo} given by equation (36).

positions of the atoms depend on the sign of α , the energy does not, as could be expected.

The numerical value of κ_{geo} has been found using the

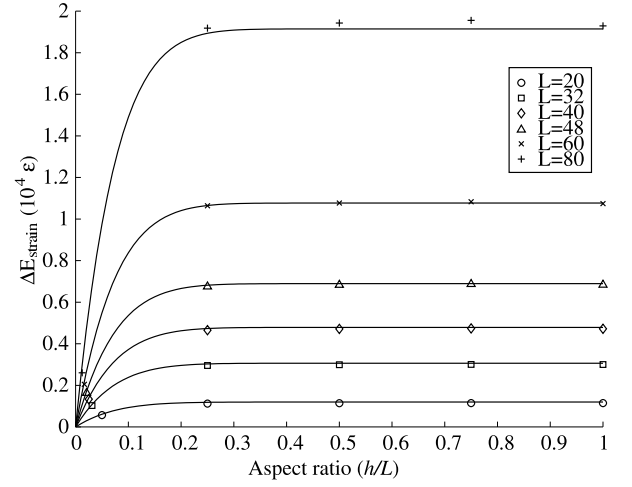


FIG. 12: Numerical data and theoretical curves for the strain energy given by (28).

displacements of the atoms of the substrate; for every system, the amplitude of the theoretical displacement field [which is close to, but not equal to Eq. (19) because of periodic boundary conditions] has been adjusted to the displacements of the substrate atoms. Figure 11 shows the agreement between the curves and the data.

Figure 12 shows the good agreement between the strain energy obtained from the simulations and the analytical expression (28). In Appendix B we elaborate on the choice of this equation.

APPENDIX B: FUNCTIONAL FORM OF EQ. (28)

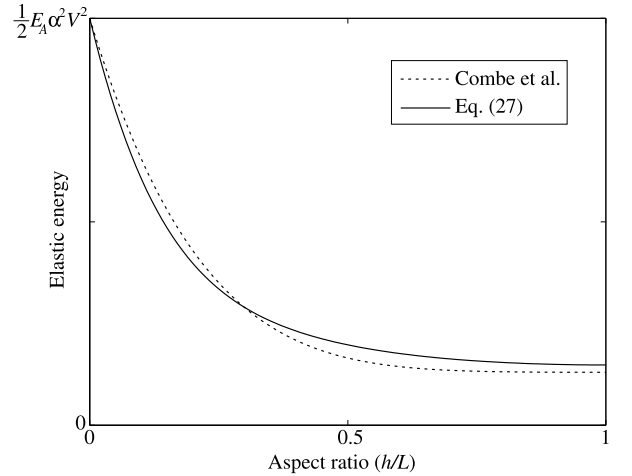


FIG. 13: Elastic energy for an island of given volume V as a function of its aspect ratio h/L .

We mentioned in Section II B 2 that a better fit to the numerical data is obtained with a function of the form $E(L, h) = C v(L, h)$ [where $v(L, h)$ has units of volume],

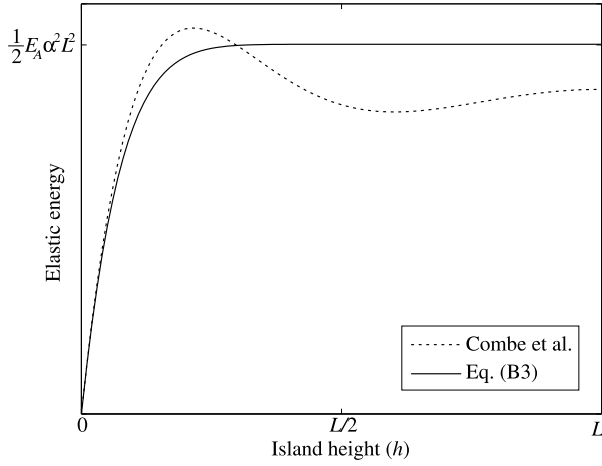


FIG. 14: Elastic energy for an island of given width L as a function of its aspect height h .

rather than $E(L, h) = CVR(h/L)$. We show here a comparison between our expression for $v(L, H)$, Eq. (27), and that used by CJB⁴; the latter is obtained by writing, first, the function $R(h/L)$ in terms of the quantities used in the present paper:

$$R_{\text{CJB}}(r) = A + Be^{-Cr/(1-r/2)}, \quad (\text{B1})$$

with $A = 0.13$, $B = 0.87$ and $C = -4.811$ and $r = h/L$. Since $v(L, h) = R(h/L)V$, it is a simple matter to connect the two functional forms. We get

$$v_{\text{CJB}}(L, h) = \frac{\sqrt{3}}{2}h(L - h/2) \left(A + Be^{-Ch/(L-h/2)} \right), \quad (\text{B2})$$

which must be compared with Eq. (27), and

$$R(r) = \frac{(1 - e^{-cr/(1-r)})}{cr(1 - r/2)}. \quad (\text{B3})$$

Figure 13 shows the the elastic energy of an island of fixed volume V as a function of its aspect ratio, according to Eqs. (B3) and (B1). The two curves are different, but their general behaviour is very similar. Note in particular that the starting points coincide and that the end points are less than 2% apart.

The situation is however very different for the elastic energy of an island of fixed width as a function of height (Fig. 14). CJB's expression for the energy yields a peak around $h/L = 0.2$ and has a minimum around $h/L = 0.6$; in contrast, our expression increases monotonically with height. Our preference for the form of Eq. (28) is mainly based on this observation and the quality of the fit to the LJ data (see Fig. 12).

* Present address: Laboratory of Atomic and Solid State Physics, Cornell University, Ithaca NY 14825, U.S.A. e-mail: thibault@physics.cornell.edu

† Electronic address: laurent.lewis@umontreal.ca

¹ B. Datta and S. Das, Appl. Phys. Lett. **56**, 665 (1990).

² D. Loss and D.P. DiVincenzo, Phys. Rev. A **57**, 120 (1998).

³ C. S. Lent, P. D. Tougaw, W. Porod, and G. H. Bernstein, Nanotechnology **4**, 49 (1993).

⁴ N. Combe, P. Jensen, and J.-L. Barrat, Surf. Sci. **490**, 351 (2001).

⁵ L.G. Wang, P. Kratzer, M. Scheffler, and N. Moll, Phys. Rev. Lett. **82**, p. 4042 (1999).

⁶ V.A. Shchukin, N.N. Ledentsov, P.S. Kop'ev, and D. Bimberg, Phys. Rev. Lett. **75**, 2968 (1995).

⁷ I. Daruka and A.L. Barabási, Phys. Rev. Lett. **79**, 3708 (1997).

⁸ Y. W. Zhang, Phys. Rev. B **61**, 10 388 (2000).

⁹ J. E. Prieto and I. Markov, in *Quantum dots: Fundamentals, Applications, Frontiers*, proceedings of NATO Advanced Research Workshop, Crete, Greece, 2003, edited by B. Joyce, P. Kelires, A. Naumovets, and D.D. Vvedensky (to be published by Klumer).

¹⁰ V.A. Shchukin and D. Bimberg, Rev. Mod. Phys. **71**, 1125 (1999).

¹¹ A. L. Barabási, Appl. Phys. Lett. **70**, 2565 (1997).

¹² H.M. Koduvally and A. Zangwill, Phys. Rev. B **60**, R2204 (1999).

¹³ K. E. Khor and S. Das Sarma, Phys. Rev. B **62**, 16657 (2000).

¹⁴ M. Meixner, E. Schöll, V.A. Shchukin, and D. Bimberg, Phys. Rev. Lett. **87**, 236101 (2001).

¹⁵ R. M. Tromp, F. M. Ross, and M. C. Reuter, Phys. Rev. Lett. **84**, 4641 (2000).

¹⁶ P. Müller and R. Kern, Microsc. Microanal. Microstruct. **8**, 229 (1997).

¹⁷ J. P. Wittmer, A. Tanguy, J.-L. Barrat, and L.J. Lewis, Europhys. Lett. **57**, 423 (2002).

¹⁸ J. Tersoff and R. M. Tromp, Phys. Rev. Lett. **70**, 2782 (1993).

¹⁹ L. D. Landau and E. M. Lifshitz, *Theory of Elasticity* (Butterworth-Heinemann, London, 1995).

²⁰ C. Ratsch and A. Zangwill, Surf. Sci. **293**, 123 (1993).

²¹ F. C. Frank, J. H. van der Merwe, Proc. R. Soc. London. Ser. A **198**, 205 (1949).

²² M. Volmer and A. Weber, Z. Phys. Chem. **119**, 277 (1926).

²³ I. N. Stranski and L. Krastanov, Sitzungsber. Akad. Wiss. Wien, Math.-Naturwiss. Klasse **146**, 797 (1937).

²⁴ Note the error in Ref. 4.